European Review for Medical and Pharmacological Sciences 2019; 23: 6570-6578

MiR-548c-3p suppressed the progression of papillary thyroid carcinoma via inhibition of the HIF1α-mediated VEGF signaling pathway

Y. DU, J. ZHU, B.-F. CHU, Y.-P. YANG, S.-L. ZHANG

Department of General Surgery, Xinhua Hospital Affiliated to Shanghai Jiaotong University School of Medicine, Shanghai, P.R. China

Abstract. – OBJECTIVE: Papillary thyroid carcinoma (PTC) is the most common type of thyroid malignancy with physiological microRNA (miR) pathomorphological changes. MiR-548c-3p participates in multiple processes of tumor development and progression. However, the role of miR-548c-3p in PTC and the underlying mechanisms remain undefined. Therefore, this study aimed to detect the expression of miR-548c-3p in PTC and to explore its exact function.

MATERIALS AND METHODS: MiR-548c-3p expression was analyzed in PTC tissue and cell lines by Real-Time fluorescence quantitative Polymerase Chain Reaction. Colony formation and cell viability assay were used to measure cell proliferation. Wound healing assay and transwell invasion assay were conducted to examine cell migration and invasion. The protein expression of the signaling pathways was determined by Western blot analysis.

RESULTS: Our results indicated that miR-548c-3p was downregulated in PTC tissues and cell lines. Moreover, miR-548c-3p mimics suppressed PTC cell viability, colony formation, cell migration, and invasion capacity. Low expression of miR-548c-3p significantly enhanced N-cadherin and vimentin expression. A negative correlation was determined between miR-548c-3p and hypoxia-inducible factor (HIF) 1α or vascular endothelial growth factor (VEGF) levels, indicating that miR-548c-3p inhibited tumor progression by suppressing the HIF1α-mediated VEGF signaling pathway.

CONCLUSIONS: MiR-548c-3p could suppress PTC progression by inhibiting the HIF1α-mediated VEGF signaling pathway.

Key Words:

Papillary thyroid carcinoma, MiR-548c-3p, Vascular endothelial growth factor, Hypoxia-inducible factor 1α, Progression.

Introduction

Thyroid cancer is a common malignant tumor in the head and neck, with an incidence rate comprising 1% of all malignant tumors[1]. Thyroid cancer incidence has surged in the past several decades, constituting 1-2% of all new tumors globally[2]. Papillary thyroid carcinoma (PTC), the major subtype, represents 80% of all malignant thyroid tumors[3]. After efficacious treatment, more than 80% of patients with PTC have 35- or 40-year survival[4,5]. Moreover, 10% of patients have disease recurrence or disease accompanied by cervical lymph node metastasis, which can lead to death[6].

Meanwhile, the recurrence and mortality of patients with PTC under traditional therapeutic measures have exhibited an increasing trend. Therefore, the molecular mechanisms of PTC progression should be explored to identify therapeutic targets. Micro-ribonucleic acids (miRNAs), which are short noncoding single-strand RNA with approximately 19-24 nucleotides in length, are highly conserved, and their specificity of dysregulation is ubiquitously detectable in all types of tumor[7]. Dysregulation of miRNAs has been implicated in various cellular processes, including cell differentiation, proliferation, migration, and apoptosis[8,9]. Multiple miRNAs, such as miR-791 and miR-613, are abnormally expressed and promote the incidence and development of PTC[10,11]. Therefore, the distinct expression features of miRNA can potentially provide a basis for the preoperative clinical diagnosis of PTC.

Although miR-548c-3p, which is obtained from miR-548c and consists of 22 nucleotides, is a less studied miRNA[12], it is closely related to various cancers, including prostate cancer, glioma, gastric cancer, and breast cancer[13-16]. Luo et al[17] found that reduced expression of miR-548c-3p in osteosarcoma contributes to cell proliferation. Tormo et al[16] indicated that miR-548c-3p plays crucial regulatory roles in breast cancer progression by inhibiting the effect of the hypoxia-inducible factor-1 alpha (HIF1α)-mediated vascular endothelial growth factor (VEGF) pathway. Notably, the HIF1α-mediated VEGF signaling pathway is also involved in central lymph node metastasis

Corresponding Author: Shenglai Zhang, Ph.D; e-mail: zshenglaish@163.com

and lateral neck lymph node metastasis, which are highly associated with unfavorable prognosis and progression of PTC[18,19]. Regardless, the underlying molecular mechanisms of miR-548c-3p via the target HIF1α-mediated VEGF signaling pathway in PTC has yet to be determined.

Thus, we hypothesized that the HIF1α-mediated VEGF signaling pathway is strengthened in case of unfavorable progression of PTC owing to the reduced expression of miR-548c-3p. This research also investigated the effects of miR-548c-3p on the prognosis and progression of PTC and explored the feasible mechanism of action.

Materials and Methods

Tissue Samples

A total of 44 PTC tissue samples (PTC tissues and the matched paracancerous thyroid tissues) were obtained from the Xinhua Hospital Affiliated to Shanghai Jiaotong University School of Medicine. These samples were pathologically confirmed to be PTC between May 2016 and May 2018. Before tumor resection, no patient received radiotherapy, chemotherapy, or immunotherapy in the aforementioned hospital. Data on the general condition of the patients included age, gender, tumor size, multifocality, lymph node metastasis, and the tumor node metastasis (TNM) classification by the International Union Against Cancer. Written informed consent from all patients and approval of this study by the Ethics Committee of Xinhua Hospital Affiliated to Shanghai Jiaotong University School of Medicine were obtained.

Cell Culture and Transfection

PTC cell lines (TPC and K1) were purchased from the Shanghai Cell Biochemical Institute. Cells were cultured in Dulbecco's Modified Eagle's Medium (Code No.11330107; Invitrogen, Carlsbad, CA, USA) with 10% fetal bovine serum (FBS; Code No. 16000044; Gibco, Grand Island, NY, USA) and 1% penicillin/streptomycin (Code No. 15140122; Gibco, Grand Island, NY, USA). Cells were maintained at 37°C ± 0.2°C in a humidified incubator with 5.0% CO_2. TPC and K1 cells were cultured in six-well plates and transfected with negative control (NC) siRNAs or miR-548c-3p by Lipofectamine 2000 (Code No. 11668019; Invitrogen, Carlsbad, CA, USA) in accordance with the instructions provided by the manufacturer. The miR-548c-3p mimics and the NC mimics were synthesized by ZoonBio Biotechnology Co., Ltd. (Nanjing, Jiangsu, China).

Cell Viability Assay

Cells were treated as previously described and seeded in a 96-well plate at a density of 1000 cells/100 μL per well with a total amount of 200 μL. After the cells were cultured for 24, 48, 72, and 96 h, cell viability was assessed using the Cell Counting Kit-8 (Code No.CK04-1; Dojindo, Kumamoto, Kyoto, Japan), and the absorbance was measured at 450 nm by using a microplate reader.

Colony Formation Assay

Cells were seeded into each well of the six-well plate and then cultured in the incubator at 37°C with 5% CO_2 and saturated humidity. After being cultured for 2 weeks, the cells fixed with methanol for 15 min by using 0.1% crystal violet (Code No. C8470, Solarbio, Tongzhou, Beijing, China) were visualized under a dissection microscope (Olympus, Tokyo, Japan), and the number of colonies consisting of 50 cells or more was determined.

Wound Healing Assay

The miR-548c-3p mimic- or NC mimic-transfected TPC or K1 cells (2×10^5-cells) were seeded into 12-well culture plates and were maintained at 90% confluence. These confluent TPC or K1 cell monolayers were then wounded by scratching with a sterilized 200 μL pipette tip. The wounded areas were visualized under a Motic AE30/31 microscope (Xiamen, Fujian, China) after scratching at 0 and 48 h.

Transwell Invasion Assay

To evaluate the effect of miR-630 on cellular migration and invasion, TPC and K1 cells (NC mimic- or miR-548c-3p mimic-transfected) resuspended in the serum-free medium were plated on the top chambers of 8 μL Costar transwell pore inserts that were pre-coated with Matrigel. After the culture with serum-free medium was starved for 24 h, the cell suspension was transferred to the apical chambers (200 mL per chamber). Cells were allowed to invade via the insert membrane. After being fixed with 95% alcohol and stained with crystal violet, the cells were photographed under a microscope (Olympus, Tokyo, Japan). The experiments were independently repeated in triplicate.

Western Blot Assay

A radioimmunoprecipitation lysis (RIPA) buffer (ComWin Biotech, Changping, Beijing, China) was applied to extract total protein from TPC and

K1 cells after treatment. After separation by 8% sodium dodecyl sulfate polyacrylamide gel (SDS-PAGE), the desired proteins were transferred to polyvinylidene difluoride membranes (PVDF; IPFL00010; EMD Millipore, Billerica, MA, USA). Primary antibodies specific to VEGF (sc-7269, 1:1,000), vimentin (sc-80975, 1:1,000), N-cadherin (sc-8424, 1:1,000), HIF1α (sc-13515, 1:1,000), and glyceraldehyde 3-phosphate dehydrogenase (GAPDH; sc-66163, 1:1,000) were applied. The samples were washed with Tris-Buffered Saline with Tween-20 (TBST) and then incubated with secondary antibodies [peroxidase-conjugated AffiniPure Goat Anti-Rabbit IgG (H + L), 1:200, ZB-2301; ZSGB-BIO, Xicheng, Beijing, China]. The gray values of the bands were quantified using the ImageJ software.

RNA Extraction and Quantitative Real Time-Polymerase Chain Reaction

The total RNA was extracted from PTC tissue samples and cell lines by using the TRIzol reagent (Code No.15596026, Invitrogen, Carlsbad, CA, USA). The extracted RNA was stored at –80 °C after measuring the concentration. Subsequently, total RNA was used in cDNA synthesis with specific primers using TaKaRa Reverse Transcription Kit (Code No. RR047A; TaKaRa, Otsu, Shiga, Japan). PCR amplification was then conducted using the SYBR Green Taq Mix (TaKaRa, Otsu, Shiga, Japan) on a Bio-Rad Real-Time PCR System (Code No. CFX96; Bio-Rad Laboratories, Hercules, CA, USA). Amplification was conducted under the following conditions: 95°C for 5 min, followed by 35 cycles of 95°C for 5 s, 60°C for 20 s, and 70°C for 10 s. Amplification reactions were performed in 96-well plates by using the 7900HT Fast Real-Time PCR System (Code No. 4346906; Applied Biosystems, Foster City, CA, USA). The $2^{-\Delta\Delta Ct}$ method was used to quantify the expression levels of miR-548c-3p. Data were normalized to the levels of U6. The PCR primers used were miR-548c-3p forward: 5'-ACACTCCAGCTGGGCAAAAATCTCAAT-3' and reverse: 5'-CTCAACTGGTGTCGTGGA-3'; U6 forward: 5'-CTCGCTTCGGCAGCACA-3' and reverse: 5'-AACGCTT CACGAATTTGCGT-3'.

Statistical Analysis

All data were expressed as mean values ± standard deviation ($\bar{x} \pm s$). Repeated-measures analysis of variance (ANOVA) were used to compare means across one or more variables that are based on repeated observations. Student's *t*-test was conducted using SPSS ver. 22.0 (SPSS Inc., Chicago, IL, USA) to compare the differences between the two groups. Correlation analysis was performed to assess the correlation between the two variables. All data were expressed using GraphPad Prism 6 (GraphPad Software, La Jolla, CA, USA, USA). Differences were considered statistically significant if $p < 0.05$.

Results

Clinicopathological Characteristics of Patients with Papillary Thyroid Carcinoma

The correlations between miR-548c-3p expression and clinicopathologic characteristics in PTC were analyzed. MiR-548c-3p expression was found to be associated with tumor size (mm) ($p<0.05$), multifocality ($p<0.05$), extrathyroidal invasion ($p<0.05$), lymphatic metastasis ($p<0.05$), and TNM stage ($p<0.001$) (Table I). Meanwhile, the age and gender ratio between the two groups showed no significant difference ($p>0.05$, Table I).

MiR-548c-3p is Downregulated in PTC Tissues and Cell Lines

The level of miR-548c-3p in PTC tissue was significantly lower than that in matched paracancerous thyroid tissues ($t=6.630$, $p<0.01$; Figure 1A). MiR-548c-3p expression in PTC cell lines, including K1 and TPC, was significantly reduced in NC mimics relative to that in miR-548c-3p mimics (TPC: $t=1.155$, $p<0.01$; K1: $t=7.821$, $p<0.01$; Figure 1B).

MiR-548c-3p Suppressed Proliferation in TPC and K1 Cells

We transfected miR-548c-3p mimics into two thyroid cancer cell lines, TPC and K1, and found that the viability of both cell lines was significantly reduced (TPC: $F=369.834$, $p<0.01$, Figure 1C; K1: $F=253.844$, $p<0.01$; Figure 1D). The up-regulation of miR-548c-3p considerably impaired the capacity of colony formation in both cell lines (TPC: $t=20.066$, $p<0.01$, Figure 1E; K1: $t=24.455$, $p<0.01$, Figure 1F).

MiR-548c-3p Repressed Migration and Invasion in TPC and K1 Cells

In contrast with the NC mimic-transfected cells, TPC and K1 cells showed inhibited migratory capacity with increased miR-548c-3p expression

Table I. Correlation between clinicopathological features and miR-548c-3p expression.

Characteristic	No. of patients [n/(%)]	$\bar{x}$±SD	*t*	*p*
Gender				
Male	17	0.55 ± 0.23	0.128	0.899
Female	27	0.56 ± 0.23		
Age (years)				
< 50	21	0.50 ± 0.23	1.603	0.116
≥ 50	23	0.61 ± 0.21		
Tumor size (mm)				
≤ 10	29	0.61 ± 0.22	2.620	0.012
> 10	15	0.43 ± 0.18		
Multifocality				
Single	20	0.65 ± 0.23	2.689	0.010
Multiple	24	0.48 ± 0.19		
Extrathyroidal invasion				
Negative	22	0.63 ± 0.20	2.260	0.029
Positive	22	0.48 ± 0.23		
Lymph node metastasis				
Negative	24	0.63 ± 0.22	2.601	0.013
Positive	20	0.46 ± 0.20		
TNM stage				
0, I, and II	25	0.64 ± 0.21	3.380	0.002
III and IV	19	0.44 ± 0.18		

(TPC: t=18.892, p<0.01, Figure 2A; K1: t=16.344, p<0.01, Figure 2B). Furthermore, the number of invaded cells was markedly smaller when they were transfected with miR-548c-3p mimics than with NC mimics (TPC: t=10.833, p<0.01, Figure. 2C; K1: t=9.720, p<0.01, Figure 2D).

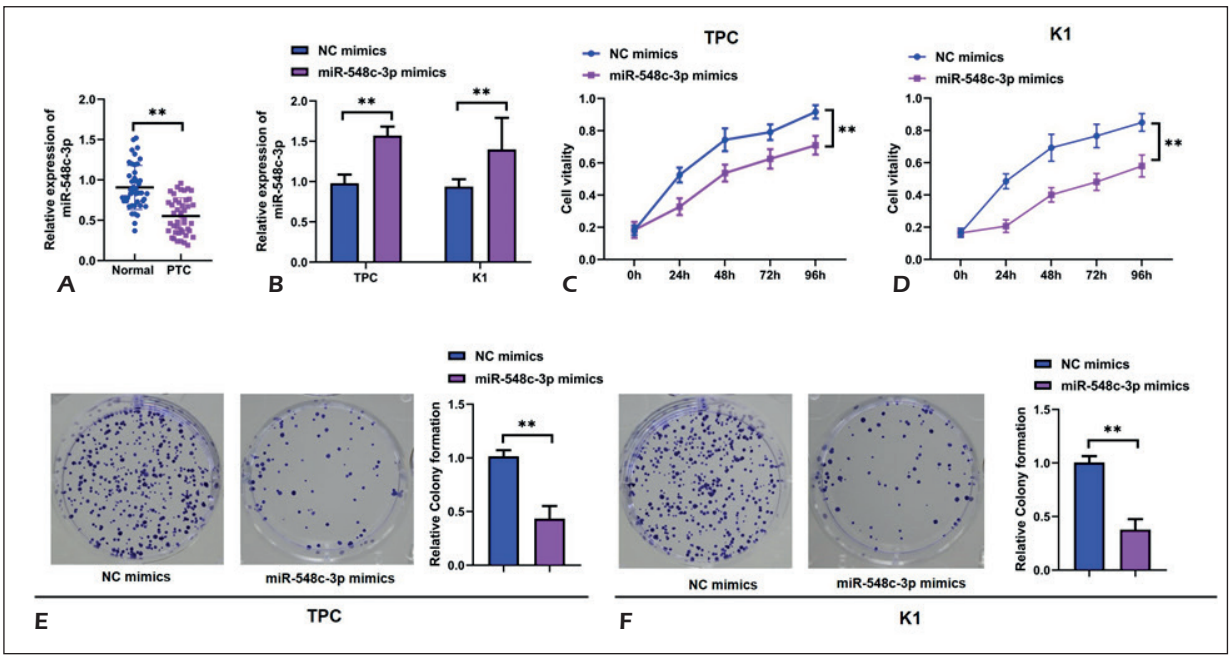

Figure 1. MiR-548c-3p was downregulated in PTC tissues and inhibited the cellular proliferation of TPC and K1 cells. ***A***, Expression of miR-548c-3p in 44 pairs of PTC tissues and matched paracancerous thyroid tissues was determined by RT-PCR. ***B***, Expression of miR-548c-3p in TPC and K1 cells was detected by qRT–PCR. ***C-D***, Cell viability of TPC and K1 cells were evaluated by CCK-8 assay. ***E-F***, Clonogenic capacity of TPC and K1 cells was assessed by cell colony formation assay. Representative images of TPC and K1 cells by photomicrographs (400×). Data represent the mean ± S.E.M. **p<0.01 was significant.

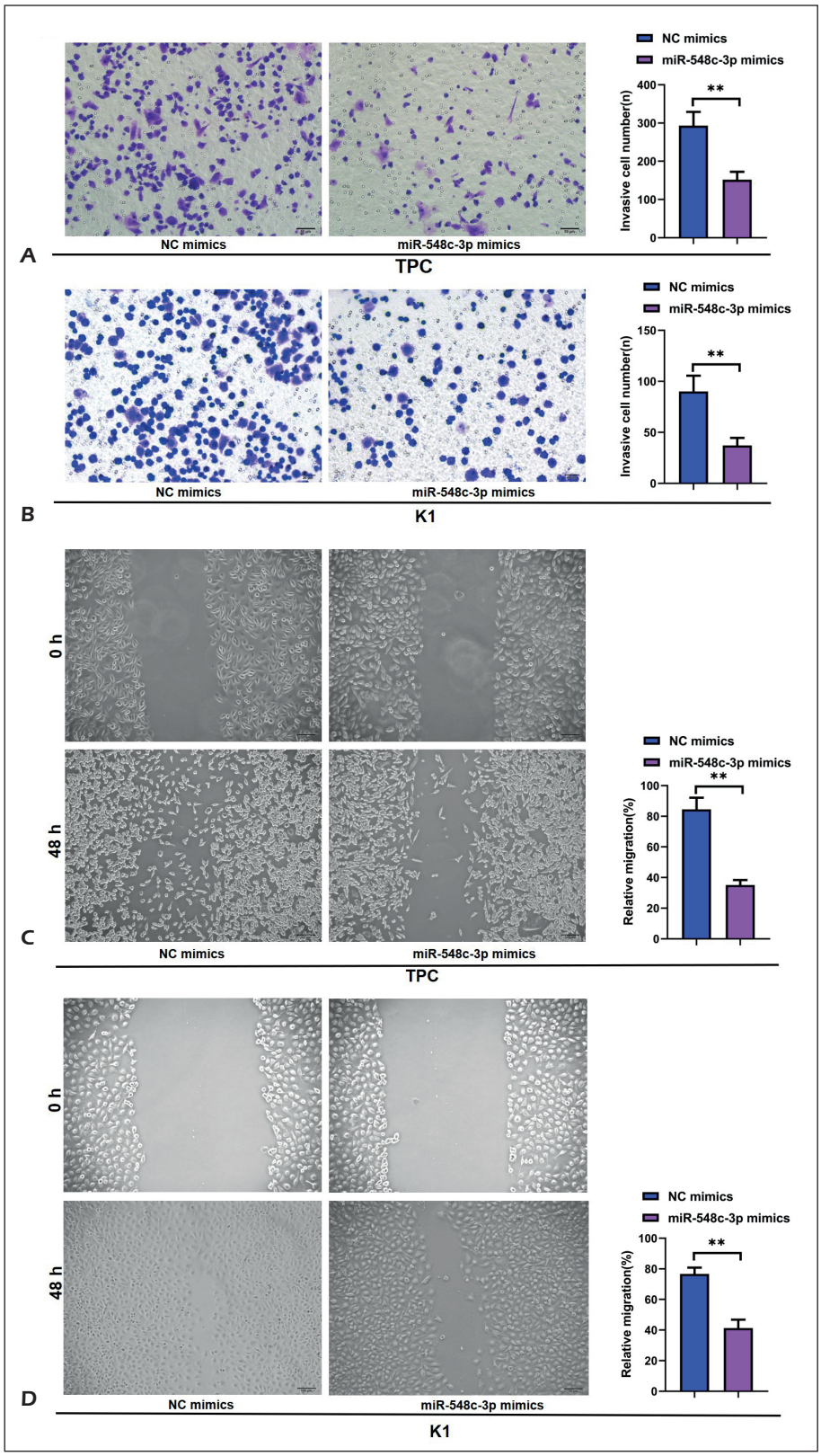

Figure 2. MiR-548c-3p inhibited the migratory and invasive capacity of TPC and K1 cells. ***A-B***, Migratory capacity of TPC and K1 cells was evaluated by wound healing assay. ***C-D***, Invasion capacity of TPC and K1 cells was evaluated by transwell invasion assay. Representative images of TPC and K1 cells by photomicrographs (400×). Data represent the mean ± S.E.M. $^{**}p<0.01$ was significant.

MiR-548c-3p Enhanced N-Cadherin and Vimentin Expression in TPC and K1 Cells

The N-cadherin and vimentin levels in TPC and K1 cells were assessed to examine whether miR-548c-3p affected the expression of epithelial-mesenchymal transition markers. After transfection with miR-548c-3p mimics, the N-cadherin (TPC: t=2.707, p<0.05, Figure 3A; K1: t=2.633, p<0.05, Figure 3B) and vimentin (TPC: t=2.517, p<0.05, Figure 3A; K1: t=2.688, p<0.05, Figure 3B) levels of these treated cells were markedly reduced relative to those of cells transfected with NC mimics.

MiR-548c-3p Repressed VEGF and HIF1α Expression in TPC and K1 Cells

The protein expression of VEGF (TPC: t=4.626, p<0.01, Figure 3C; K1: t=2.688, p<0.05, Figure 3D) and HIF1α (TPC: t=5.307, p<0.01, Figure 3C; K1: t=4.158, p<0.01, Figure 3D) was significantly increased in miR-548c-3p mimics relative to those in NC mimics. Meanwhile, miR-548c-3p expression and VEGF expression (TPC: r^2=0.7185, p<0.01, Figure 3E; K1: r^2=0.8452, p<0.01, Figure 3G) exhibited a significant inverse correlation, an inverse association between miR-548c-3p and HIF1α expression (TPC: r^2=0.6794, p<0.01, Figure 3F; K1: r^2=0.5833, p<0.05, Figure 3H) in TPC and K1 cells.

See also Data Supplementary file

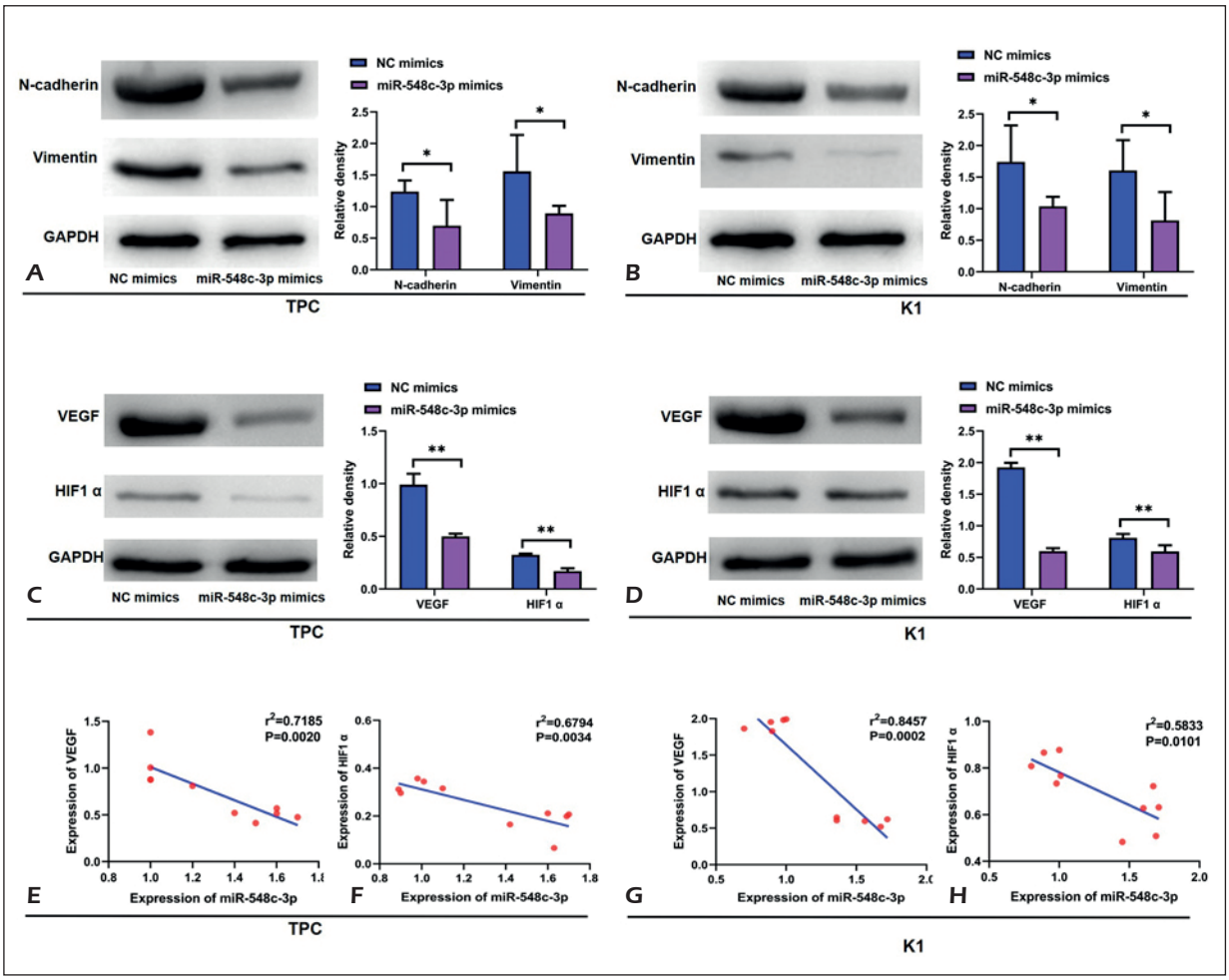

Figure 3. MiR-548c-3p suppressed the expression of N-cadherin and vimentin and the activity of the HIF1α-mediated VEGF signaling pathway. ***A-B***, Expression of N-cadherin and vimentin in TPC and K1 cells was determined by Western blot assay. ***C-D***, Expression of VEGF and HIF1α in TPC and K1 cells was examined by Western blot assay. ***E-F***, Correlation between miR-548c-3p level with VEGF and HIF1α protein levels in TPC. G, H, Correlation between miR-548c-3p level with VEGF and HIF1α protein levels in K1. Data represent mean ± S.E.M. **p<0.01 or *p<0.05 were significant.

Discussion

In the present report, 44 PTC tissue samples (PTC tissues and matched paracancerous thyroid tissues) were evaluated. We determined that miR-548c-3p was significantly downregulated in PTC tissues, indicating the antitumor effects of this miRNA in PTC. Subsequently, miR-548c-3p expression was significantly downregulated in TPC and K1 cells. A further analysis of the biological functions of miR-548c-3p indicated that this molecule could suppress the proliferation, migration, and invasion of PTC cells, functioning as an antitumor factor. Notably, the results also indicated that upregulation of miR-548c-3p directly repressed metastasis by inhibiting the expression of the HIF1α–VEGF signaling pathway. Overall, our findings revealed that miR-548c-3p served as a tumor suppressor in PTC progression by suppressing the HIF1α–VEGF signaling pathway. This study is the first which determines the expression, function, and mechanism of action of miR-548c-3p in PTC.

An increasing number of studies[13-16] proved that downregulation of miR-548c-3p facilitated the progression of several tumors and could be used as biomarkers and therapeutic targets. In the current work, 44 fresh pathological tissue specimens of PTC were collected. QRT–PCR results revealed that miR-548c-3p was poorly expressed in PTC tissues, particularly in patients with tumor size >10 mm, multifocality ($p<0.05$), extrathyroidal invasion ($p<0.05$), lymphatic metastasis ($p<0.05$), and TNM stages III and IV. This finding suggested that miR-548c-3p exhibited potential as a biomarker for evaluating PTC prognosis and could also play a role in metastasis, which was not investigated in this research.

Colony formation and wound-healing assay also showed that transfection of miR-548c-3p mimics markedly decreased cell vitality and colony formation. This result demonstrated that miR-548c-3p overexpression significantly reduced the proliferation and colony formation capacity of tumor cells, functioning as an antitumor factor. Meanwhile, the upregulation of miR-548c-3p inhibited migratory capacity and invasion, suggesting that miR-548c-3p could act as a negative regulator in the metastatic progression of PTC. N-cadherin and vimentin, as epithelial-mesenchymal transition markers in tumor invasion and metastasis[20,21], were overexpressed in both NC mimic-transfected PTC cells and could be downregulated by miR-548c-3p. This process provides the underlying explanation of PTC inhibition by miR-548c-3p via the reduction of N-cadherin and vimentin expression.

HIF1α, an oxygen-sensitive transcription factor, enables the transcription of multifarious proangiogenic cytokines such as VEGF[22]. Novel evidence of HIF1α-mediated VEGF abundance being controlled by miRNA has been presented[23,24]. Reports[25-27] have demonstrated that the HIF1α-mediated VEGF signaling pathway is activated during the progression of thyroid cancer, particularly in cervical lymph node metastasis. However, the underlying molecular mechanisms of miR-548c-3p on the HIF1α-mediated VEGF signaling pathway in PTC have yet to be determined. The present work, which elucidates the biological functions of miR-548c-3p, is the first to identify the inverse association between miR-548c-3p expression and the HIF1α-mediated VEGF signaling pathway in the PTC cell line, which is an avenue for further research to explore potential therapeutic treatment for PTC.

Referring to the relevant literature, we found that the accumulation of HIF1α under ischemic and hypoxic conditions contributed to the inhibitory effect of degradation mediated by ubiquitination, which was controlled by miRNA[23]. VEGF could stimulate the growth of blood vessels and metastasis of cervical lymph nodes, further promoting tumor development and metastasis[28-30]. Thus, the downregulation of the HIF1α-mediated VEGF signaling pathway is the crucial mechanism underlying miR-548c-3p suppression of migration and invasion. This molecule could also regulate cell proliferation and colony formation in TPC in the current study. However, Lu et al[14] reported that miR-548c-3p inhibited glioma cell proliferation and migration by downregulating the proto-oncogene c-Myb. Luo et al[17] found that miR-548c-3p could directly inhibit the 3'-untranslated region of integrin αv to prevent osteosarcoma tumor growth. These related pathways of miR-548c-3p for suppressing PTC was not investigated in the present study and will be explored in future research.

Conclusions

We offer an insight into the low expression of miR-548c-3p in PTC tissues and cell lines. MiR-548c-3p inhibited PTC cell proliferation, invasion, and migration via the downregulation of the HIF1α-mediated VEGF signaling pathway. With biological and clinical implications for PTC, this research provides novel targets for the diagnosis and biotherapy of PTC.

Funding

This work was supported by the Important Program of Shanghai Municipal Health Bureau (Grant no. 20124015) and the Bureau Awards of Shanghai Municipal Health Bureau (Grant no. 054058).

Conflict of Interests

The Authors declared that they have no conflict of interests.

References

1) Siegel RL, Miller KD, Jemal A. Cancer statistics, 2018. CA Cancer J Clin 2018; 68: 7-30.
2) Gimm O, Castellone MD, Hoang-Vu C, Kebebew E. Biomarkers in thyroid tumor research: new diagnostic tools and potential targets of molecular-based therapy. J Thyroid Res 2011: 631593.
3) Lim H, Devesa SS, Sosa JA, Check D, Kitahara CM. Trends in thyroid cancer incidence and mortality in the United States, 1974-2013. JAMA 2017; 317: 1338-1348.
4) Zhu Z, Gandhi M, Nikiforova MN, Fischer AH, Nikiforov YE. Molecular profile and clinical-pathologic features of the follicular variant of papillary thyroid carcinoma. An unusually high prevalence of ras mutations. Am J Clin Pathol 2003; 120: 71-77.
5) Cui L, Zhang Q, Mao Z, Chen J, Wang X, Qu J, Zhang J, Jin D. CTGF is overexpressed in papillary thyroid carcinoma and promotes the growth of papillary thyroid cancer cells. Tumour Biol 2011; 32: 721-728.
6) Bai Y, Kakudo K, Nakamura M, Ozaki T, Li Y, Liu Z, Mori I, Miyauchi A, Zhou G. Loss of cellular polarity/cohesiveness in the invasive front of papillary thyroid carcinoma and periostin expression. Cancer Lett 2009; 281: 188-195.
7) Wightman B, Ha I, Ruvkun G. Posttranscriptional regulation of the heterochronic gene lin-14 by lin-4 mediates temporal pattern formation in C. elegans. Cell 1993; 75: 855-862.
8) Bartel DP. MicroRNAs: target recognition and regulatory functions. Cell 2009; 136: 215-233.
9) Shukla GC, Singh J, Barik S. MicroRNAs. Processing, maturation, target recognition and regulatory functions. Mol Cell Pharmacol 2011; 3: 83-92.
10) Gao XB, Chen CL, Tian ZL, Yuan FK, Jia GL. MicroRNA-791 is an independent prognostic factor of papillary thyroid carcinoma and inhibits the proliferation of PTC cells. Eur Rev Med Pharmacol Sci 2018; 22: 5562-5568.
11) Qiu W, Yang Z, Fan Y, Zheng Q. MicroRNA-613 inhibits cell growth, migration and invasion of papillary thyroid carcinoma by regulating SphK2. Oncotarget 2016; 7: 39907-39915.
12) Cheng H, Hu P, Wen W, Liu L. Relative miRNA and mRNA expression involved in arsenic methylation. PLoS One 2018; 13: e0209014.
13) Rane JK, Scaravilli M, Ylipää A, Pellacani D, Mann VM, Simms MS, Nykter M, Collins AT, Visakorpi T, Maitland NJ. MicroRNA expression profile of primary prostate cancer stem cells as a source of biomarkers and therapeutic targets. Eur Urol 2015; 67: 7-10.
14) Lu J, Zhang M, Yang X, Cui T, Dai J. MicroRNA-548c-3p inhibits T98G glioma cell proliferation and migration by downregulating c-Myb. Oncol Lett 2017; 13: 3866-3872.
15) Chang H, Kim N, Park JH, Nam RH, Choi YJ, Lee HS, Yoon H, Shin CM, Park YS, Kim JM, Lee DH. Different microRNA expression levels in gastric cancer depending on Helicobacter pylori infection. Gut Liver 2015; 9: 188-196.
16) Tormo E, Pineda B, Serna E, Guijarro A, Ribas G, Fores J, Chirivella E, Climent J, Lluch A, Eroles P. MicroRNA profile in response to doxorubicin treatment in breast cancer. J Cell Biochem 2015; 116: 2061-2073.
17) Luo Z, Li D, Luo X, Li L, Gu S, Yu L, Ma Y. Decreased expression of miR-548c-3p in osteosarcoma contributes to cell proliferation via targeting ITGAV. Cancer Biother Radiopharm 2016; 31: 153-158.
18) Lv Y, Sun Y, Shi T, Shi C, Qin H, Li Z. Pigment epithelium-derived factor has a role in the progression of papillary thyroid carcinoma by affecting the HIF1alpha-VEGF signaling pathway. Oncol Lett 2016; 12: 5217-5222.
19) Jang JY, Kim DS, Park HY, Shin SC, Cha W, Lee JC, Wang SG, Lee BJ. Preoperative serum VEGF-C but not VEGF-A level is correlated with lateral neck metastasis in papillary thyroid carcinoma. Head Neck 2019 Mar 7. doi: 10.1002/hed.25729. [Epub ahead of print]
20) Bhandari A, Zheng C, Sindan N, Sindan N, Quan R , Xia E , Thapa Y, Tamang D, Wang O, Ye X, Huang D. COPB2 is up-regulated in breast cancer and plays a vital role in the metastasis via N-cadherin and Vimentin. J Cell Mol Med 2019. May 22. doi: 10.1111/jcmm.14398. [Epub ahead of print]
21) Zhang QY, Men CJ, Ding XW. Upregulation of microRNA-140-3p inhibits epithelial-mesenchymal transition, invasion, and metastasis of hepatocellular carcinoma through inactivation of the MAPK signaling pathway by targeting GRN. J Cell Biochem. 2019 May 1. doi: 10.1002/jcb.28750. [Epub ahead of print]
22) Birner P, Schindl M, Obermair A, Plank C, Breiteneckker G, Oberhuber G. Overexpression of hypoxia-inducible factor 1alpha is a marker for an unfavorable prognosis in early-stage invasive cervical cancer. Cancer Res 2000; 60: 4693-4696.
23) Li L, Wang M, Mei Z, Cao W, Yang Y, Wang Y, Wen A. LncRNAs HIF1A-AS2 facilitates the up-regulation of HIF-1alpha by sponging to miR-153-3p, whereby promoting angiogenesis in HUVECs in hypoxia. Biomed Pharmacother 2017; 96: 165-172.
24) Li LJ, Huang Q, Zhang N, Wang GB, Liu YH. MiR-376b-5p regulates angiogenesis in cerebral ischemia. Mol Med Rep 2014; 10: 527-535.
25) Lan L, Luo Y, Cui D, Shi BY, Deng W, Huo LL, Chen HL, Zhang GY, Deng L. Epithelial-mesenchymal transition triggers cancer stem cell generation in human thyroid cancer cells. Int J Oncol 2013; 43: 113-120.

26) Koperek O, Bergner O, Pichlhöfer B, Oberndorfer F, Hainfellner JA, Kaserer K, Horvat R, Harris AL, Niederle B, Birner P. Expression of hypoxia-associated proteins in sporadic medullary thyroid cancer is associated with desmoplastic stroma reaction and lymph node metastasis and may indicate somatic mutations in the VHL gene. J Pathol 2011; 225: 63-72.
27) Huang XQ, He WS, Zhang HQ, Yang R, Huang T. Relationship between expression of vascular endothelial growth factor and cervical lymph node metastasis in papillary thyroid cancer: a meta-analysis. J Huazhong Univ Sci Technolog Med Sci 2017; 37: 661-666.
28) Ribatti D, Annese T, Ruggieri S, Tamma R, Crivellato E. Limitations of anti-angiogenic treatment of tumors. Transl Oncol 2019; 12: 981-986.
29) Li Y, Huang P, Peng H, Yue H, Wu M, Liu S, Qin R, Fan J, Han Y. Antitumor effects of Endostar(rh-endostatin) combined with gemcitabine in different administration sequences to treat Lewis lung carcinoma. Cancer Manag Res 2019; 11: 3469-3479.
30) Gao Y, Qian H, Tang X, Du X, Wang G, Zhang H, Ye F, Liu T. Superparamagnetic iron oxide nanoparticle-mediated expression of miR-326 inhibits human endometrial carcinoma stem cell growth. Int J Nanomedicine 2019; 14: 2719-2731.